# Development of a Microsensor to Minimize Post Cataract Surgery Complications

M. Mottaghi, F. Ghalichi, H. Badri Ghavifekr, and H. Niroomand Oskui

*Abstract*—This paper presents design and characterization of a microaccelerometer designated for integration into cataract surgical probe to detect hardness of different eye tissues during cataract surgery. Soft posterior lens capsule of eye can be easily damaged in comparison with hard opaque lens since the surgeon can not see directly behind cutting needle during the surgery. Presence of microsensor helps the surgeon to avoid rupturing posterior lens capsule which if occurs leads to severe complications such as glaucoma, infection, or even blindness. The microsensor having overall dimensions of 480 μm x 395 μm is able to deliver significant capacitance variations during encountered vibration situations which makes it capable to distinguish between different types of tissue. Integration of electronic components on chip ensures high level of reliability and noise immunity while minimizes space and power requirements. Physical characteristics and results on performance testing, proves integration of microsensor as an effective tool to aid the surgeon during this procedure.

*Keywords*—Cataract surgery, MEMS, Microsensor, Phacoemulsification.

## I. INTRODUCTION

CATARACT removal, involving an ultrasonic cutting technique called phacoemulsification, is one of the most common minimally invasive surgical procedures practiced around the world. In this technique the hard, opaque human lens is fragmented by a sharp, ultrasonically driven cutting needle. Because the surgeon cannot see directly under the hollow titanium or stainless steel cutting needle as the lens is fragmented and aspirated, the underlying and much softer posterior capsule is sometimes unintentionally ruptured. The very fragile posterior capsule is easily cut in comparison with the hard protein molecules composing the lens. A tear usually requires considerable time to repair and invariably leads to complications such as glaucoma, infection, and sometimes blindness. The complication rate of this procedure is highly dependent on the skill and experience of the surgeon. To address this problem a microsensor utilizing MEMS technology designed to help the surgeon in identifying tissue hardness during this procedure that requires delicate cutting. The method to identify tissue hardness is by monitoring amplitude and/or frequency of the ultrasonic vibrating system on the surgical cutting tool. The system can warn the surgeon when a hard-to-soft material transition which is characteristic of the lens-to-posterior capsule transition, is taking place.

The emphasis is on detection of type and hardness of the tissue the surgeon is cutting, rather than exact monitoring of vibrating system. To the best of our knowledge, there has been only one case of microsensor integration into phaco (phacoemulsification) handpiece in order to detect tissue hardness, which is done by biomedical engineering department, university of Minnesota, USA. They designed a piezoelectric sensor (force transducer) and inserted it directly behind the cutting needle. Their physical sensing method relies on direct detection of the impressed loading on the needle presented by the lens with the help of piezoelectric sensor. They successfully tested it on 252 patients [1].

Since the sensor is placed exactly behind cutting needle, it blocks irrigation flow; to compensate this, it is necessary to modify the whole handpiece case with adding another fluid input after force transducer. In our approach the miniature sensor is designed such that it can be easily integrated into phaco probe without slightest change in probe case which proves to be more practical and cost effective. Since proposed sensor fits perfectly into vibrating part of the probe, it dose not make any blockage in pathway of irrigation flow, eliminating the need for additional fluid input.

## II. MECHANICAL DESIGN OF SENSOR

Every phaco handpiece utilizes a piezoelectric crystal as source of vibration. Operating frequency of this crystal for studied phaco machine was 40 kHz with 100 μm total phaco tip displacement [2]. Many other phaco machines share the same or have similar specifications [3]. For every single degree of freedom vibratory system formed of a body of mass *m,* a spring of stiffness *k* and a damper of viscosity *c,* actuated by an external force defined as (1). The dynamic equation of motion would be (2), general solution of (2) is sum of a
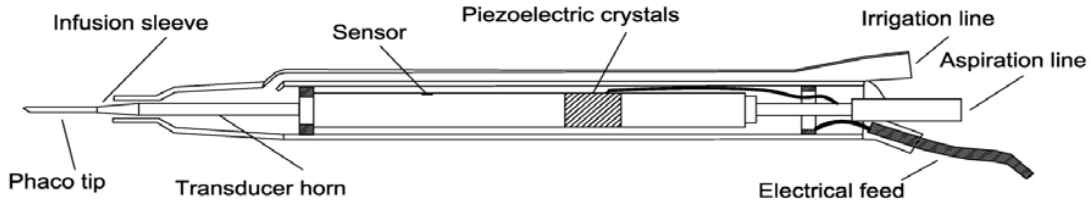
Fig. 1 Cross-sectional view of a typical phacoemulsification handpiece with integration of proposed sensor

complementary or homogeneous solution (which describes the system's vibration at the natural frequency) and a particular or steady-state solution.

$$f(t) = F \sin(\omega t) \qquad (1)$$

$$m\ddot{x} + c\dot{x} + kx = f(t) \qquad (2)$$

Where $F$ is amplitude and $\omega$ is oscillating frequency of external force. The particular solution (which describes the forced response of a vibratory system and generally analyzed in the frequency domain by studying its amplitude and phase angle) can be written as (3).

$$x_p(t) = X \sin(\omega t - \varphi) \qquad (3)$$

$$X = \frac{X_{st}}{\sqrt{(1 - \frac{m\omega^2}{k})^2 + (\frac{c\omega}{k})^2}} \Rightarrow \frac{X}{X_{st}} = \frac{1}{\sqrt{(1 - \beta^2)^2 + (2\xi\beta)^2}} \qquad (4)$$

Where $x(t)$ is particular solution of (2), $X$ is amplitude of response, $\varphi$ is phase angle, $X_{st}$ is static displacement and defined as $F/K$, $\beta$ is frequency ratio and $\xi$ is damping ratio. The plot of (4) indicates that for vibratory systems with small frequency ratio, damping and damping ratio have little effect on overall behavior of the system. Therefore response amplitude of vibration will not reduce significantly when viscous damping effects are considered [4].


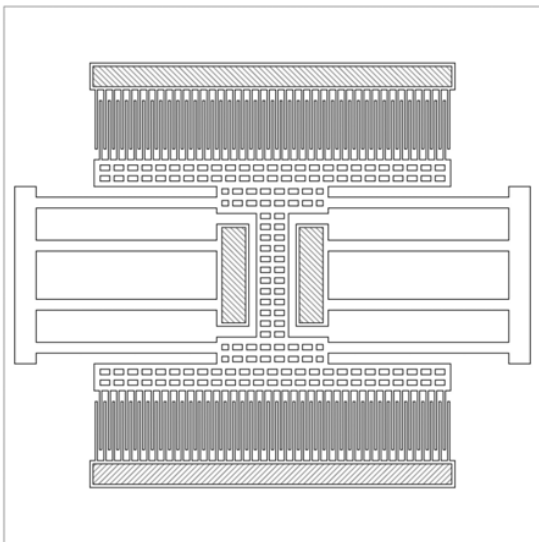
Fig. 2 CAD layout of sensor structure with static combs. Dimensions of surrounding square are 500 μm x 500 μm. Hatched area indicate anchors

Considering mentioned parameters, design criteria of structure were as follows: I. Overall dimension should not exceed 500 μm x 500 μm, leaving enough space for integrated electrical components. II. Should deliver enough capacitance so variations are measurable, at least 0.1 pF. III. Resonance frequency should be 3-4 times of operating frequency which yields 5-10 μm displacement between static and movable comb fingers. IV. Designated anchors should be big enough to not only withstand applied stresses during vibration but ensures failure free operation for many years considering hysteresis stresses, fatigue phenomenon and safety factors.

Dealing with ultrasonic frequencies leads us to a structure much like a resonator in terms of design. However major difference is resonators operate at their resonance frequency (β=1) whereas accelerometers have much lower frequency ratio [5]. CAD layout of structure is shown in Fig. 2. Etching holes help to reduce mass as much as possible without sacrificing structure robustness, beside their main role during fabrication process. Calculated natural frequency of structure based on poly-silicon mechanical properties ($E = 169$ Gpa, $\upsilon = 0.22$) is about 140 kHz which is 3.5 times of operating frequency. This leads to frequency ratio of β = 0.286. Important geometric dimensions are listed in Table I.

TABLE I
GEOMETRIC PARAMETERS

| Quantity | Dimension (μm) |
|---|---|
| Total length | 480 |
| Total width | 395 |
| Length of each finger | 55 |
| Width of each finger | 2 |
| Thickness of fingers | 10 |
| Initial gap forming (right) | 2 |
| Initial gap forming (left) | 2 |
| Length of initial overlaid coupling fingers | 45 |

Energy loss phenomena in microdevices can generally be grouped into two large categories: One group includes losses that are produced by fluid-structure interaction (slide film damping-squeeze film damping) [6] and the other group contains loss mechanisms that are generated through intrinsic (material) dissipation, which also referred to as mechanical noise mechanisms [7]. Analytical solution for calculation of air viscous damping yields to damping ratio of 4.87E-5. Therefore, presence of air as a viscous fluid almost has no effect in reducing response amplitude of system in comparison with ideally vacuumed environment. For more accurate results stokes flow of fluid above and damping between the comb fingers, in addition to couette flow, are considered [8].

Although material dissipations are subject of special importance in resonators, for structures with very low frequency ratio, these losses so small that do not considered [9]. Plot of (4) with constant value of $\xi$ is shown in Fig. 3. Amplitude ratio of 1.088 indicates there will be 8.8 μm changes in distance between each pair of comb fingers as oscillation takes place with 100 μm amplitude.
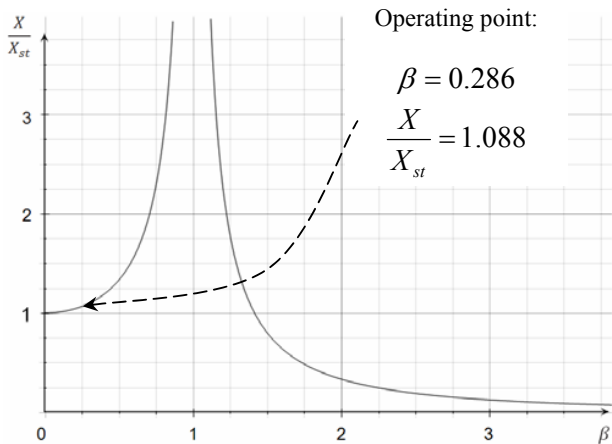


Operating point:

$$\beta = 0.286$$

$$\frac{X}{X_{st}} = 1.088$$

Fig. 3 Amplitude ratio versus frequency ratio

### III. CAPACITANCE MODELING OF SENSING STRUCTURE

The sensing part is based on capacitance variations in two comb units with total capacity of 0.165 pF on each side in stationary situation. As dynamic structure (shuttle) moves forth and back to static combs, the capacitance variations versus displacement show slight nonlinearity. During vibration, total variation of capacitance is 0.075 pF which is 45.4 % of stationary status value; that is not surprising since high g accelerometers usually show great capacitance variations. Because detection and ability to distinguish between three vibration situations are main purpose of sensor design, nonlinear behavior of capacitance variations is not much of concern.
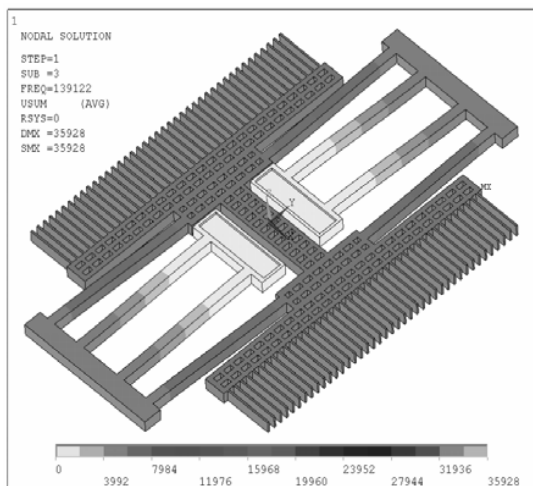


Fig. 4 FEA is used to extract modal shapes and natural frequencies of structure

### IV. ON CHIP ELECTRICAL COMPONENTS

Overall low capacitance of system requires integration of electronic capacitance measurement with signal conditioning circuit board on sensing chip. Surface micromachining enables integration of electronic components which has its own advantages: less power consumption, smaller space requirement, enhanced reliability and great immunity to noise and distortion. Design of this electronic system based on CMOS technology is done in cooperation with electrical engineering department.

Fig. 5 shows a simplified view of the accelerometer with its integrated electronic circuit for signal conditioning. The input is first and second ports in sensor block that are connected to two fixed comb anchors, the third port is connected to anchors of moving comb and acts as output of sensor. The two capacitors are connected in series and form a capacitive divider. The two inputs into the device are driven differentially by a 1 MHz square wave, generated by an oscillator. Ideally, the values of the capacitors are equal in stationary status and the amplitudes of the square waves on each capacitor are equal but with 180° phase difference. In this situation, two signals cancel each other at the common summing node and the output voltage to the amplifier is mean value of square wave (dc voltage). When acceleration takes place, the floating plate moves and changes the values of the sensor capacitors oppositely, this produces a signal at the summing node which is proportional to the amount of deflection.
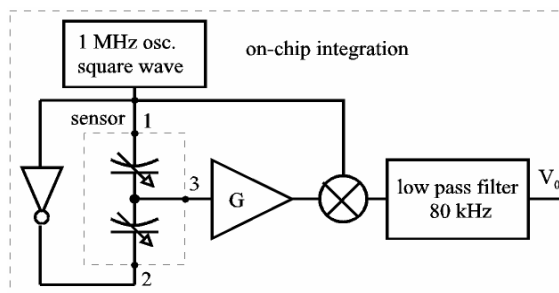


Fig. 5 Block diagram of the accelerometer sensor with its integrated electronic circuit for signal conditioning

### V. FABRICATION PROCESS AND PACKAGING

Designated fabrication process is standard surface micromachining with 2 μm pitch. Major processes as shown in Fig. 6 include: deposition of silicon oxide layer on Silicon wafer which itself is coated with very thin layer of silicon nitride. This process is done with "Low Pressure Chemical Vapor Deposition" (LPCVD) technique, then photo-lithography of deposited layer (a). Etching and structuring of silicon oxide layer and deposition of polysilicon layer with previous method (LPCVD) (b). Photolithography of deposited polysilicon then etching and structuring of mentioned layer with "Deep Reactive Ion Etching" (DRIE) process. Total 10 μm thickness of structure can be achieved with this method (C). Wet chemical etching of sacrificial layer (silicon oxide) with hydrofluoric acid (HF), which completes fabrication of

structure (d). During this process etching holes enhance removal process of silicon oxide layer.
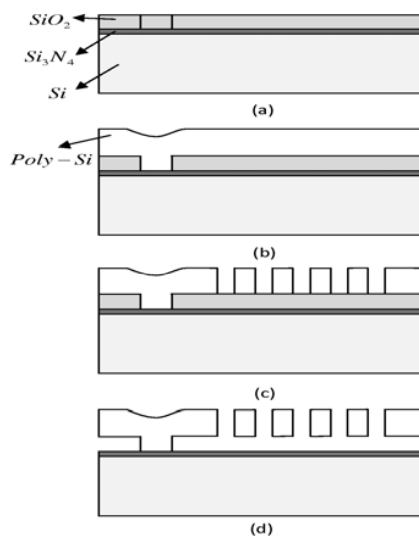


Fig. 6 Microstructure fabrication processes

Packaging of the system includes covering above of sensor with Pyrex glass which along with substrate at the bottom restricts vertical movements of vibrating structure. All components are fixed and encapsulated in designated place with resin. Overall dimensions of whole system (sensing chip with packaging) will not exceed 3 mm x 3 mm x 1 mm. Accelerometers unlike many other types of sensors such as pressure, chemical, etc. do not re1y on direct contact with sensing environment for their operation. This enables packaging to isolate the sensor completely from surroundings which enhances overall system's durability and reliability. Since the system operates in normal pressure and temperature, no special materials and techniques are used in this process.
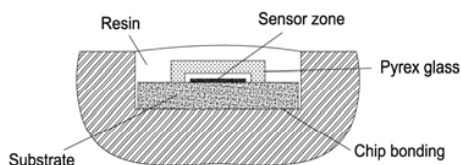


Fig. 7 Schematic view of sensing chip with packaging components

## VI. TEST SETUP AND RESULTS

Test setup includes design of electrical circuit equivalent to mechanical sensor coupling with integrated electronic circuit. Response of piezoelectric actuator to three input load curves is shown in Fig. 8. During the cataract removal, three different vibration statuses driven by piezoelectric crystals can be recognized: the handpiece is idle and there is no load on vibrating cutting needle (A). The cutting needle is fragmenting hard and opaque lens (B) and when the cutting needle is rupturing soft posterior lens capsule (C). Although during first transition (A to B), there is a noticeable drop in frequency and amplitude, there is not the same amount of difference in second transition (B to C).

With the aid of signal processing, signal amplification is higher when second transition occurs; hence second and third situation become more distinguishable. If and when the cutting needle advances the very hard, brittle and calcified cataract past into the soft posterior capsule; the vibrating blade stops and surgeon will be notified. Since there is no published data about hardness of different eye tissues, clinical calibration of system is crucial.
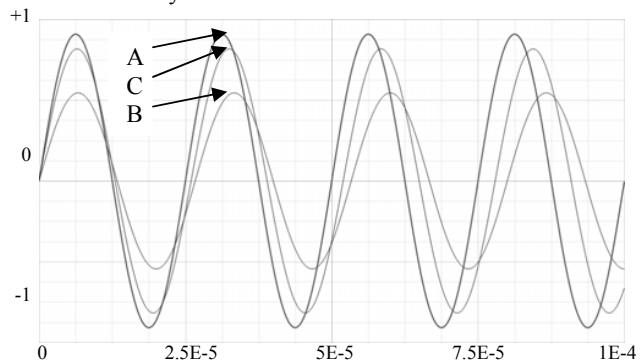


Fig. 8 Amplitude and frequency of output signal for three vibration situations

## VII. CONCLUSION

In conventional phaco machines there is no sensing mechanism for detection of tissue hardness which leaves successful operation solely based on surgeon skills. Severe complications of posterior lens capsule rupture, emphasize on necessity of such systems inclusion into surgical probe to minimize post operational complications. Such detection mechanism based on real world considerations is designated with design of a microsensor and development of all belonging components. It is demonstrated that integration of a sensor based on MEMS technology into a surgical tool enables surgeon to get real-time feedback on the type of tissue he is cutting. This represents a relatively new application for MEMS technology.

## REFERENCES

[1]   Polla, D. L., Erdman, A. G., Robbins, W. P., Markus, D. T., Diaz-Diaz, J., Rizq, R., Nam, Y.,Brickner, H.T., Krulevitch, P., and Wang, A., 2000, "Microdevices in Medicine", *Ann Rev of Biomed Eng*, 2:552-572.
[2]   Optikon "Pulsar2 minimal stress" series, Optikon Inc, Available: http://www.optikon.com
[3]   Alcon Inc, Available: http://www.alcon.com , Bausch & Lomb Inc, Available: http://www.bausch.com
[4]   C. F. Breads, *Structural Vibration: Analysis and Damping*, New York: John Willy & Sons Inc, 1996, pp. 47-52.
[5]   Lobontiu, N. O., *Mechanical Design of Microresonators*, New York: McGraw HILL, 2004, pp. 3-22.
[6]   J. B. Starr, "Squeeze-film damping in solid-state accelerometers", *Technical Digest, IEEE Solid State Sensor and Actuator Workshop,* 1990, pp. 44–47.
[7]   T. W. Roszhart, "The effect of thermoelastic internal friction on the $Q$ of micromachined silicon resonators", *Technical Digest on Solid-State Sensor and Actuator Workshop*, 1990, pp. 13–16.
[8]   X. Zhang and W. C. Tang, "Viscous Air Damping in Laterally Driven Microresonators," *Sensors and Materials*, v. 7, no. 6, 1995, pp.415-430.
[9]   A. N. Cleland, and M. L. Rourkes, "Noise processes in nanomechanical Resonators", *Journal of Applied Physics*, 92(5), 2002, pp. 2758–2769.